

Measurement Techniques for Estimating Critical Speed of Drivelines

Robert J. White, John Deere Product Engineering Center, Waterloo, Iowa

Several analytical tools exist for estimating a driveshaft's critical speed, from simple elementary beam theory to sophisticated FEA models. Ultimately, nothing is better than a test, because no one will argue with the outcome from a well-designed measurement. Impact response measurements are easy, but they tend to overpredict the critical speed. A test that sweeps the shaft speed up until failure is telling, but the speed causing failure strongly depends on even small amounts of variation in rotor unbalance. Waterfall plots of shaft displacement measurements offer the best indication of critical speed; however, sometimes the resonance isn't unmistakable or multiple resonances exist, making the critical speed unclear. A method less susceptible to system variation is offered here, fitting shaft orbit measurements to the theoretical single-degree-of-freedom equation. The procedure is to first make an impact response measurement using an accelerometer and modal hammer, then select a maximum speed for the speed sweep several hundred rpm below the resonance. A test is then run with a slow-speed sweep up to the previously determined maximum speed and then back down while measuring the shaft's deflection with displacement transducers. The radii of the orbits are computed, and the orbit radius vs. shaft speed is plotted. The single-degree-of-freedom equation parameters are adjusted to fit these data, resulting in estimates for critical speed, damping, unbalance to stiffness ratio and an offset (half static runout).

In rotating machinery, there is a dynamic phenomenon called critical speed that is known to cause catastrophic driveline failures. At the critical speed, the lateral bending frequency of the rotor-shaft assembly is equal to the rotation frequency, resulting in very large radial displacement. This article examines drivelines, so the assumption that the shaft is very soft compared with the bearings and housing is reasonable. If the bearings and housings were soft compared with the shaft, as in short shafts, then at the first two critical speeds the shaft would bounce and pitch as a rigid beam.¹ The displacement may become so great that any of a number of failure modes are experienced; however, the classic critical speed failure mode is shaft buckling (Figure 1).

A rotating shaft bows like a jump rope. As its speed increases, its displacement increases. The force tending to displace the shaft comes from its unbalance. All shafts have some unbalance, so no shaft, no matter how well balanced, is immune to critical speed failure. While the displacement response has all the properties of a resonance, the deflection is DC, that is, a strain gage placed on the shaft records a strain offset. While a single bending gage will indicate a DC offset as the shaft rotation speed approaches the critical speed, unless the experimenter is unfortunate enough to have the shaft deflect in the plane that puts the gage on the shaft's neutral axis, two bending bridges are required to measure the full bending effect, because the shaft's plane of deflection in an axisymmetric shaft is unknown.

As the speed is further increased toward the critical speed, the deflection continues to increase until the shaft yields or buckles. Secondary damage may be much more serious than the shaft failure, because broken rotors at high speeds contain a lot of energy and have the potential to do serious damage as they throw themselves. While there are certain applications that operate at speeds above the critical speed, generally speaking, it is imperative that the designer avoid running at critical speed.²

In this article, critical speed is introduced, giving way to a frequency response function. Various failure modes are described and



Figure 1. Critical speed failure of driveshaft that resulted in buckling failure.

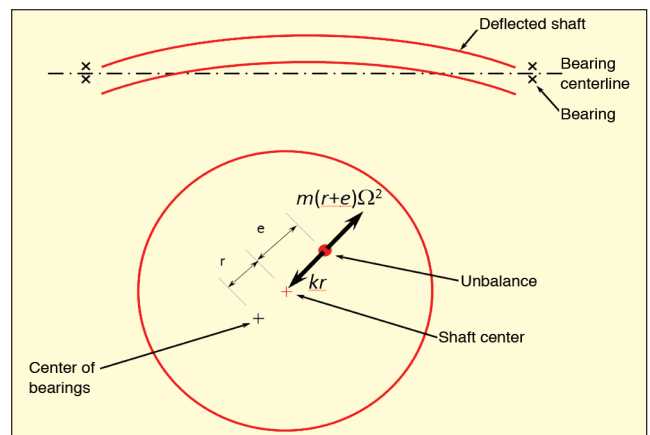


Figure 2. Shaft deflection due to centrifugal force acting on unbalance assumed to be halfway between bearings; upper image shows the shaft deflection due to unbalance, while lower image is crosssection midway between bearings showing centrifugal force due to unbalance and shaft stiffness that acts as restoring force.

some design guidelines are provided. There are various methods for estimating the critical speed, both analytically and experimentally. The analytical methods are briefly introduced, and then the experimental methods are more thoroughly discussed. We introduce a method that makes use of the shaft deflection measurements taken during a speed sweep up close to the critical speed, then fit the theoretical frequency response function to those measurements. One of the four parameters of the curve-fit model is critical speed.

Frequency Response Function

As stated above, a simply supported shaft rotating at speeds approaching the critical speed bows like a jump rope, first flexure mode. While several shaft layouts are possible, the derivations here are for the simply supported beam, because the focus here is the critical speed of drivelines. The force that causes the deflection is the unbalance inherent to technical parts. Unbalance can come from a number of sources, such as castings or forgings that are not fully machined, welded tubes, bent shafts and assembly clearances. Figure 2 shows a shaft in its deflected state. The equations derived here are for a simply supported shaft with the unbalance midway between the bearings. The derivation follows that of Den Hartog.³

Based on a paper presented at the SAE Noise and Vibration Conference, Grand Rapids, MI, June 12-15, 2017.

Summing the forces in the free body diagram of Figure 2 and making the substitution of $\omega_n^2 = \sqrt{k/m}$ along with some simple algebra, produces:

$$r = \frac{e\Omega^2}{\omega_n^2 - \Omega^2} \quad (1)$$

where:

- r = rotor radial deflection
- Ω = shaft rotation speed
- e = eccentricity of center of mass from center of shaft
- m = rotor mass (unbalance = me)
- k = shaft-bending stiffness
- ω_n = bending natural frequency

From this equation, it is plain to see that when the rotation frequency is equal to the bending natural frequency, the deflection goes to infinity. This is defined as the critical speed and is given the designation Ω_n . Another arrangement of the same equation more clearly shows how radial deflection is influenced by unbalance:

$$r = \frac{CU \Omega^2}{1 - \left(\frac{\Omega}{\Omega_n}\right)^2} \quad (2)$$

where:

- C = shaft compliance ($1/k$)
- U = shaft unbalance (me)

When damping is added to the system, the equation takes on the form found in Shigley:⁴

$$r = \frac{CU \Omega^2}{\sqrt{\left[1 - \left(\frac{\Omega}{\Omega_n}\right)^2\right]^2 + \left(2\zeta \frac{\Omega}{\Omega_n}\right)^2}} \quad (3)$$

where:

- ζ = damping ratio

This is very similar to the frequency response equation that we will be using for estimating the critical speed based on shaft deflection measurements. Its general shape is shown in Figure 3.

Failure Modes

Depending on the slenderness ratio, the shaft can fail in buckling or simply yield. Periat and Hickey demonstrate how comparing the slenderness ratio to the inflection point joining the Johnson and Euler column buckling formulae identifies whether a shaft approaching critical speed will yield or buckle.⁵ Once the shaft fails, secondary damage can be much more severe than the shaft failure itself. Shafts rotating at high speed and suddenly unrestrained easily fail their connections. Loose shafts take to flight, having so much energy that they can do serious damage to what they strike.

Other failure modes due to operating too close to the critical speed are the result of high unbalance forces, high displacements or high slope at the shaft connections. These then result in spline wear, excessive vibration, bearing failure, interference with nearby objects and/or noise.

Design Guidelines

The SAE design guideline suggests that the maximum operating speed be less than 75-85% of the critical speed calculated by the elementary beam-theory method.¹ This guideline provides a wide girth from the critical speed, because the elementary beam-theory equation it uses is only accurate if the shaft resembles a simply supported plain beam. To be clear, it should be an extremely rare event that one gets close to the critical speed, because the damage can be so devastating.

If a more accurate value of critical speed can be obtained, then one does not need as wide a safety zone, because for shafts with little damping, one can get very close to the critical speed before getting into trouble. In our experience in running drivelines to catastrophic failure, failures occurred at about 98% of the critical speed estimated by the curve-fit method to be introduced. Applying plenty of headroom then allows safe operation to about 90% of the actual critical speed. For this reason, it behooves one to obtain an accurate estimate of critical speed. While a safety zone is impera-

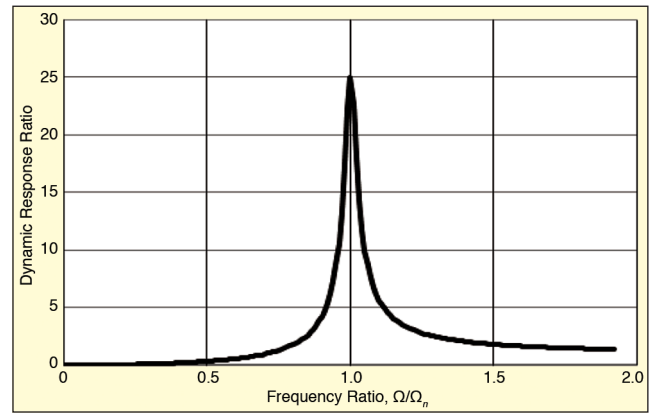


Figure 3. Frequency response function with unbalance as excitation (2% damping).

tive, it can be costly, and one should not make it unnecessarily wide. How close one designs critical speed to the maximum speed depends on how much control one has over the operating speed.

Damping

The amplitude at critical speed is highly dependent on damping ratio. Most steel drivelines have very little damping and consequently experience near certain failure at critical speed. One might assume that one countermeasure to critical speed is to add damping. Damping material is often put inside tube drivelines (e.g. foam or cardboard) to reduce the response to torsional, higher-order bending, and shell vibration modes.⁶ For critical speed, however, damping is rarely a viable alternative.

Damping occurs when kinetic energy is converted to heat. This requires relative motion and either Coulomb friction or viscous damping. Because the first bending mode of a driveline is a DC phenomenon, there is no relative motion, and opportunity for damping is minimal. Furthermore, methods used to add damping generally add mass and therefore lower critical speed.

Methods for Estimating Critical Speed

There are several ways to estimate a rotor's critical speed by analysis and measurement:

- Elementary beam-theory equation
- Finite-element analysis
- Impact response
- Identify resonance in waterfall plot
- Curve-fit measured deflection
- Ramp up speed to ultimate failure

Each of these is examined subsequently, but our recommendation for a new design would use the first five methods, in this order. The elementary beam theory is for the back of the envelope analysis at the onset of a new design. FEA is then used to confirm the design, especially if the shaft departs from the simply supported beam assumptions. If the maximum driveline speed is far enough below the critical speed, no testing is required except perhaps for confirmation. Once hardware is available, an impact response measurement identifies the shaft's first natural frequency. The actual critical speed is at or below this speed, because the modal hammer might not excite the bearings and housing, only the shaft. Spinning the shaft while measuring shaft deflection or housing vibration near the bearings accommodates methods 4 and 5. The waterfall is inspected for resonances; the critical speed appears as a resonance in the waterfall plot. Fitting the dynamic response equation, which comes from Eq. 3, to the displacement measurements provides the best estimate for critical speed. Rarely should one use the last method and run the shaft to failure.

Elementary Beam Theory. When first approaching a critical speed problem, the simplest approximation makes use of the equation seen in References 1 and 7:

$$f_n = \frac{\pi}{2} \sqrt{\frac{EI}{mL^4}} = \frac{\pi}{8} \sqrt{\frac{E(D^2 + d^2)}{\rho L^4}} \quad (4)$$

where:

f_n = first bending natural frequency

E = modulus of elasticity

I = area moment of inertia

D = shaft OD

d = shaft ID

m = mass per unit length

ρ = shaft density

L = length between the end supports

This calculation is exact for simple beams and provides a good starting point for most drivelines. The two underlying assumptions for this equation are that the shaft be a beam of constant section and that the supports are pivots at the ends of the shaft. This equation is less useful for telescoping drivelines, because they don't meet the constant section criterion. End conditions are assumed to be pivots but need not be spherical bearings or universal joints. Even a little clearance in spline connections allows the necessary slope at the supports to satisfy the simply supported assumption.

Notice in Eq. 4 that length has the most influence; however, it is usually a given in driveline layouts, and there is very little available adjustment. Modulus to density ratio (E/ρ) is important, but cost generally dictates the use of steel. The remaining design parameters are the shaft ID and OD. Notice that making the wall section thicker (reducing ID) reduces critical speed, because the mass per unit length increases more than the lateral stiffness. Consequently, when one must increase critical speed, it almost certainly implies an increase in shaft OD. This equation also assumes the beam's bearing supports are infinitely stiff, not a bad assumption for many driveline applications, but recognize that actual support stiffness will reduce the critical speed and possibly introduce bounce and pitch modes. This equation overpredicts critical speed.

Another point to notice from Equations 3 and 4 is that unbalance does not change the critical speed. It only changes the amplitude of shaft deflection at any given speed.

The beam's effective length changes with different end conditions. Equation 4 is for a simply supported beam; that is, the shaft is free to pivot at the ends. Certain other boundary conditions effectively shorten the shaft. These are found in References 8 and 9 in their sections on buckling beams.

Finite-Element Analysis. A finite-element analysis is invaluable for rotors that cannot be approximated as elementary beams or are made up of multiple materials. A simple, linear analysis is appropriate for tight connections; a more complex nonlinear analysis is necessary to handle clearances such as in spline joints. In FEA analyses, the boundary conditions (bearing and housing stiffnesses) can be properly included, providing a more accurate estimate of critical speed. An advantage of the FEA approach comes from the ability to provide relative deflection amplitudes and bearing forces for various distributions of unbalance. Once the shaft speed gets close to the critical speed, however, the amplitudes are so dependent on the damping (an educated guess at best) that the absolute amplitudes and forces are not reliable. Nonetheless, this approach is very helpful for *A to B* comparisons. A modal analysis and forced response in an automotive 4WD example is demonstrated in Ref. 10.



Figure 4. Rail magnet has two magnetic rails and stabilizes itself on round shaft much like a vee-block.

Impact-Response Method.

The impact-response method is particularly attractive, because it is fast and easy; but it requires that hardware be available. An accelerometer is placed on a rail magnet (Figure 4) on the driveline, somewhere toward the center, then a modal hammer is used to tap on the shaft in a direction parallel to the accelerometer. Several frequency responses should be averaged together; check coherence to be sure the data are consistent.

Coherence should be greater

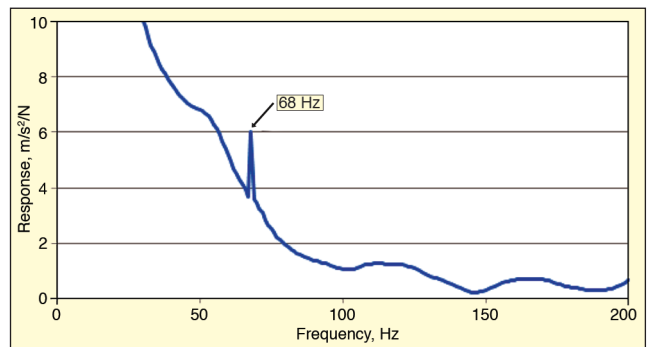


Figure 5. Frequency response of driveline; excitation from modal hammer and response measured with accelerometer.

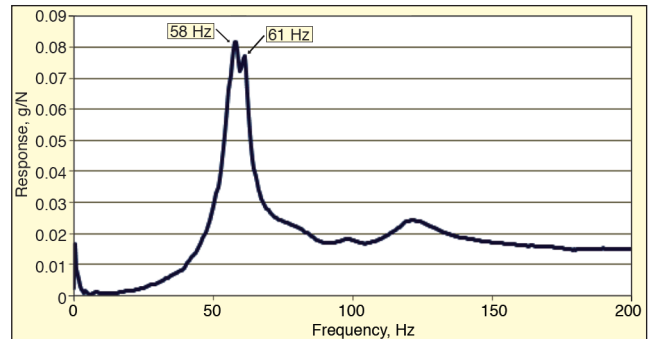


Figure 6. Two different natural frequencies were observed on this shaft when tapped in orthogonal orientations; tapping in 45° plane showed both (orbit plot for this shaft is shown in the far right plot of Figure 9).

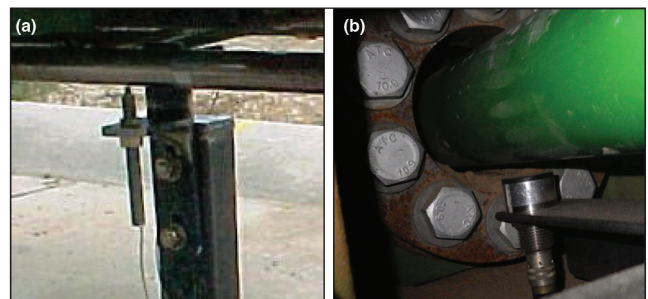


Figure 7. (a) Two eddy-current sensors measure vertical and horizontal deflection of driveshaft; sensor making vertical measurement is readily seen, while horizontal sensor mostly hidden by the driveshaft. (b) Single, much larger eddy-current sensor is used on shaft because that shaft's deflections are much greater and circular.

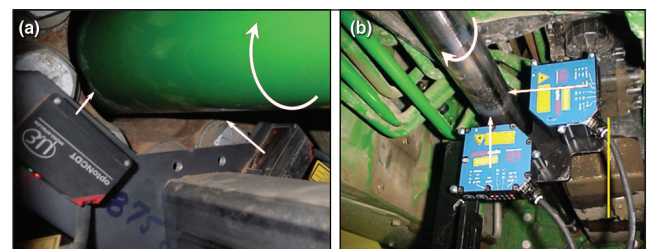


Figure 8. Two setups using triangulation lasers mounted orthogonally to measure driveline whirl during speed sweeps.

than 0.8 in the region of resonance. The impact response shown in Figure 5 has a spike at 68 Hz. The frequency resolution on this plot is 1 Hz, which means the critical speed is no more than 4080 rpm with resolution of 60 rpm. The narrowness of the spike suggests that there is little damping. That means one can get very close to the critical speed without getting into trouble; however, getting too close may be disastrous.

Use the frequency of the impact response spike as an upper limit on critical speed. Actual critical speed will be somewhat less. This upper limit can be used to determine the upper speed limit for spinning the shaft in a speed sweep. Choose a maximum speed for the speed sweep about 90% of the impact response resonance speed.

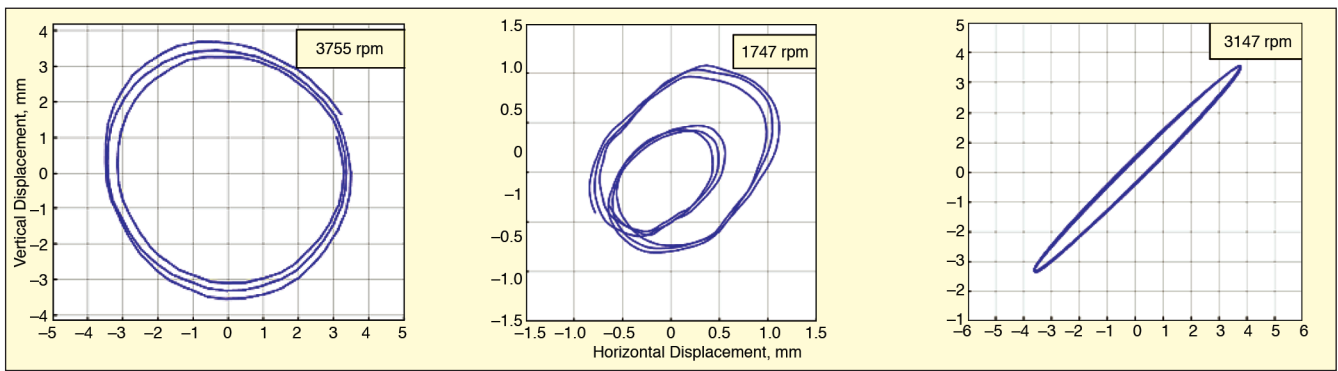


Figure 9. Measured orbits of three different drivelines (three revolutions each). Shaft in middle plot had more natural ellipse shape at speeds above and below this particular rotational speed but made this shape at half critical speed, excited by twice per rev of the U joints. Shaft in right plot had impact response shown in Figure 6.

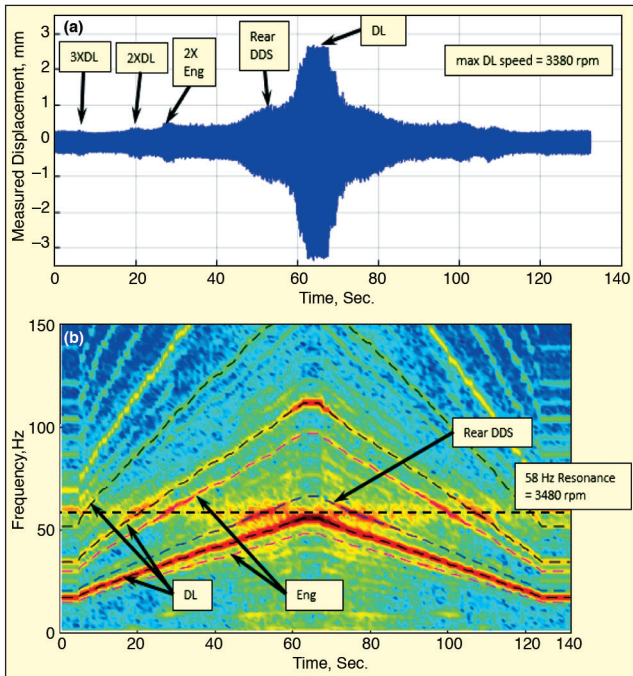


Figure 10. Time-domain plot above and waterfall plot below of shaft deflection measurements (vertical displacement only) highlight the 58 Hz resonance that is the critical speed of the driveshaft.

Asymmetrical stiffness in the housings, bearings or shaft will result in two resonance frequencies, so the impact response should be measured in at least two planes in case there are important differences in the bending natural frequencies (Figure 6). The lower frequency resonance is the first critical speed. Reference 3 discusses how two different natural frequencies result in flattened ellipses such as the one shown in Figure 9.

Instrumented Speed Sweeps. The next easiest thing is to measure acceleration at the bearings on either end of the shaft. While sometimes useful, it is far better to measure shaft displacement. Favorite displacement transducers are eddy current (inductive) sensors and triangulation lasers as shown in Figures 7 and 8. Position the transducers to measure the whirl of the driveshaft. This is most easily done by mounting them orthogonally, but if space constraints don't allow, they may be placed obliquely and the whirl can be computed by the necessary transformation.

Based on the available real estate for mounting the transducers, they are often not in the natural horizontal and vertical orientations (y and z axes). The typical ground vehicle coordinate system is +x axis is forward, +y axis is left and +z axis is up. One should perform a coordinate transformation at the data acquisition system if necessary so that the real-time orbit plots are in a coordinate system readily recognized while the test is running. The shape of the orbit plot will generally be an ellipse, but sometimes the shape is far more interesting (see Figure 9). The ellipse orientation is determined by the stiffnesses of the bearings and housings

in orthogonal directions. Once the shape of the ellipse is known, one may be able to make subsequent measurements using a single transducer.

The shaft speed should be swept over as wide a speed range as reasonable. Since you want to get very close to the critical speed without failing the driveline, target an upper speed limit in the neighborhood of 90% of the impact response resonance discussed above. During the speed sweep, monitor the ellipse size and stop increasing shaft speed when the displacement exceeds some allowable limit. After evaluating the frequency response plot to be discussed later, one might choose to repeat the test with a higher speed limit. It is far better to creep up on the maximum speed than to fail the shaft.

Acceleration and displacement data from the speed sweeps are analyzed by means of waterfall plots. A string of high-amplitude spots at a constant frequency as indicated by the broken line in Figure 10 identifies the critical speed. These natural frequencies tend to be more readily apparent in the shaft displacement measurements than the acceleration data. Acceleration waterfalls sometimes show several resonances, complicating matters. Resonances are more readily identified when several excitation sources cross it. In Figure 10, harmonics of driveline speed and engine speed help to provide clarity for determining the resonance.

When a single displacement transducer is used, an order slice through the waterfall plot at the first order of driveline speed provides a frequency response curve similar to Figure 3. When two displacement transducers are used to measure the orbit ellipse, orbit y, z measurements are converted to orbit radii and are plotted against shaft speed to create the frequency response curve. Finally the modified frequency response equation is curve fitted to the measured frequency response data:

$$r = \frac{CU \Omega^2}{\sqrt{\left[1 - \left(\frac{\Omega}{\Omega_n}\right)^2\right]^2 + \left(2\zeta \frac{\Omega}{\Omega_n}\right)^2}} + r_0 \quad (5)$$

where:

Ω = shaft speed

r = orbit radius

Ω_n = critical speed

CU = product of shaft compliance and unbalance

ζ = damping ratio

r_0 = offset (half the runout at zero speed)

This equation is the theoretical frequency response equation (Eq. 3) with one modification, the addition of the offset, r_0 . This offset accounts for the fact that technical parts are not without static runout, while the theoretical function presumes zero runout at zero speed. The measured radii are the r values, and Ω are their associated shaft speeds. The remaining parameters are solved in the curve-fitting process.

Procedure

A MATLAB script centers the ellipse on the origin, converts the y,z coordinates to distances from the origin and then takes segments of data (150 to 500 msec long) and computes the greatest

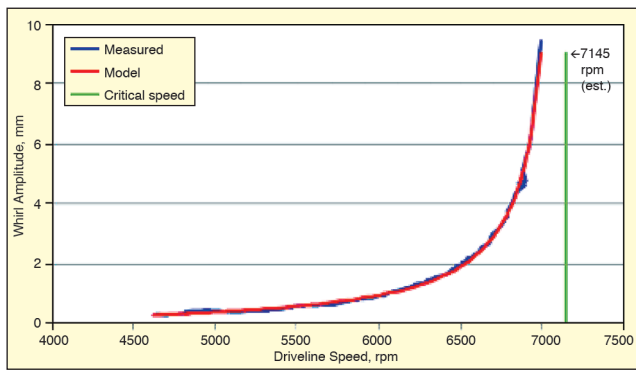


Figure 11. Orbit ellipse radii plotted vs. driveline speed; model in red was compared to entire measurement dataset in blue.

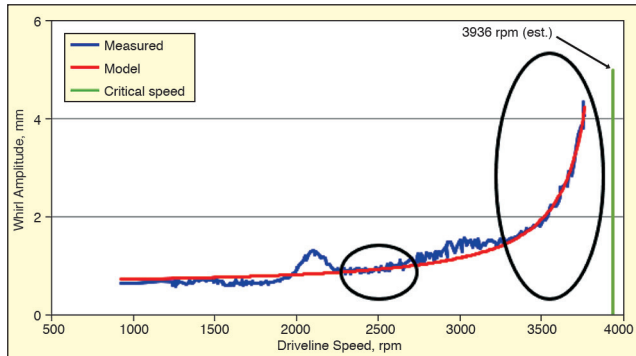


Figure 12. Orbit ellipse radii plotted vs. driveline speed; model was only fit in regions indicated by ellipses and resonance responses at about 2200 and 3000 rpm were ignored.

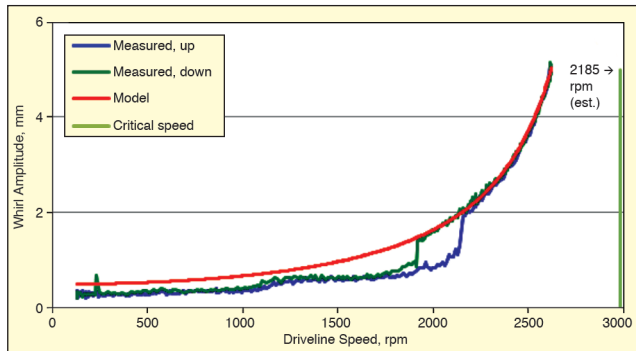


Figure 13. Orbit ellipse radii plotted vs. driveline speed; blue curve indicates sweep up, and green curve indicates the sweep down; only portion to right of jump was used to define model.

radius during that time interval. The average speed is calculated over that same interval. The length of the interval determines the speed resolution of the frequency response curve and is adjusted according to the ramp rate of the speed sweep. Longer intervals tend to cause smoothing, but at a loss of speed resolution.

The speed sweep data, that is the driveline speed and maximum ellipse radii, are saved into an Excel file where Solver can be employed to perform the curve fit. Two columns are added, one for the model's displacement and another for the difference between the measured ellipse radii and the model's displacement, the residuals. Solver is a handy optimization tool that can minimize the sum of the squares of the residuals by adjusting values for the four unknowns of Eq. 5 (Ω_n , CU , ζ and r_0). The evolutionary solving method works well. This method requires upper and lower constraints on each of the four parameters to be solved. Specify the critical speed limits about ± 2000 rpm from the critical speed estimated by the impact response or waterfall analysis. Specify the damping ratio between 0 and 0.2, CU between 0 and 0.001 mm-sec² and an offset between 0 and 1 mm. Solver then interrogates the solution space and returns with a best fit. If Solver pushes up against any of these limits, they are easily modified. Wider limits result in longer solution time. Run Solver several times to guarantee

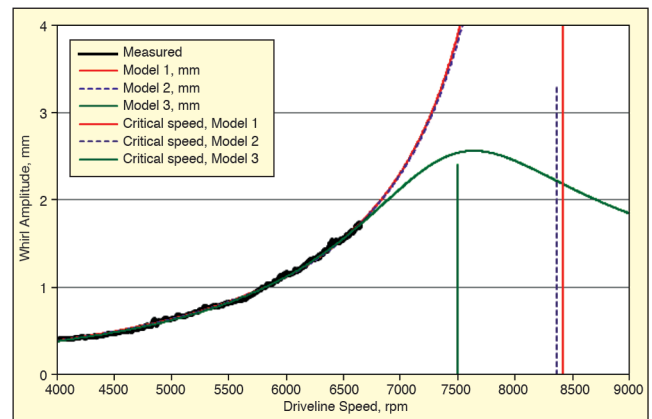


Figure 14. Three curve-fit models go through measured data (black) very well, but with very different critical speeds; red curve has 1% damping, while broken purple curve has 4% damping; green curve has 13.5% damping.

the best solution.

Figures 11, 12 and 13 show examples of how the curve-fit technique was employed on three different drivelines. These examples also show that in certain circumstances only selected portions of the measured data are used. In Figure 11, all the data were used for the curve fit. The measured data shown in Figure 12 were much like the data of Figure 10, where the shaft deflection responded to several excitation sources crossing the resonance, resulting in responses at 2200 and 3000 rpm. Only those portions indicated by the ellipses were used for the curve fit.

Figure 13 shows a nonlinear dataset. The blue curve indicates the sweep up and the green curve indicates the sweep down. By ramping in both directions, the jump separation due to nonlinearity is readily apparent. In this dataset, only the portion to the right of the jump was used to define the model. Sweeping in both directions also clearly indicates whether the shaft has yielded.

Caveat

Fitting measured shaft deflection data to the theoretical frequency response curve as introduced here is one more tool for estimating the critical speed of a driveline. While it is useful, one must use a critical eye. An example of how it can lead to misleading results is illustrated below.

When the maximum speed of the measurement is too far from the critical speed, multiple solutions to the frequency response equation (Eq. 5) can fit the measured data very well. Of course Solver will report the one that fits best, minimizing the sum of the squares of the residuals, but several may be very good fits nonetheless.

Figure 14 shows three very good curve fits on the same measured data, and Table 1 shows the parameters that define the models. The clue that the Model 3 was incorrect is the damping ratio – 13.5% damping is unreasonable. Steel drivelines tend to have very little damping. Sometimes it becomes necessary to narrow the limits on ζ to prevent Solver from selecting a solution with too much damping. Forcing lower damping values generated Models 1 and 2. While shaft deflection at 1% and 4% damping is very different at the critical speed, there is no difference in the range of these measurements. Critical speed is affected – but only slightly.

Ramp Up to Ultimate Failure. Running to ultimate failure is not recommended as a method for determining critical speed. Foremost, it can be dangerous. The events of failure include increasing deflection until the shaft breaks in two, then the unconstrained shafts tend to swing out radially and make even greater unbalance forces on the shaft ends, bearings and housings. Even before the

Table 1. Parameters defining three curve fits of Eq. 5 to the measured shaft deflection data shown in Figure 14.

	Model 1	Model 2	Model 3
Ω_n	8415 rpm	8367 rpm	7500 rpm
CU	1.27e-6 mm-sec ²	1.26e-6 mm-sec ²	1.05e-6 mm-sec ²
ζ	1%	4%	13.5%
r_0	0.10 mm	0.10 mm	0.13 mm

shaft fails, vibration levels may become extremely high and cause bearing or housing failures. The increased unbalance forces at the ends of the shafts sometimes cause the universal joints or other shaft connections to fail, and then parts go flying. These parts have a lot of energy and can do significant damage. Containment of the driveline is imperative to run this sort of test safely, but at the same time, must not be so constraining that the shaft is restrained from deflection.

Shaft buckling failure is caused by excessive stress and strain that depend directly on the amount of unbalance. That means the natural part-to-part unbalance variation and the unbalance variation due to assembly variation cause the speed at which failure occurs to also vary.

Running to failure also begs the question, What is failure? Is it when a bearing becomes noisy or when the rolling elements are ejected or does the shaft have to break in two? Is it failure when the shaft yields without buckling?

Summary

Several methods for estimating the critical speed of drivelines have been presented: two analytical methods and four making use of measurements on real parts. The two analytical methods are the elementary-beam theory (Eq. 4) and FEA. Of the measurement methods, the last method given is running a speed sweep to failure. While it seems reasonable that if one wants to know at what speed a shaft fails, then it should be run to failure, this is strongly discouraged – it can be dangerous – the results are highly variable, and the definition of failure is not universal.


The first measurement method listed is impact response. It is quick and easy and should always be done even when the waterfall or curve-fit methods are to be used. The critical speed from the impact response method provides the upper speed limit for speed sweeps employed by the waterfall and curve-fit methods. The waterfall and curve-fit methods make use of measured shaft deflection, while the shaft is slowly swept up in speed. The upper speed limit is determined by the maximum allowable deflection

and the bending natural frequency from the impact response.

In the waterfall method, a resonance line is often observed – this line is the critical speed. In some instances, either the line doesn't show itself or there are multiple resonances. In those cases, the theoretical unbalance frequency response equation (Eq. 5) can be fit to the measured data. Two of the parameters solved are critical speed and damping.

Regarding the curve-fit method, a word of warning was issued for those cases where the speed sweep doesn't come close enough to the critical speed and then multiple models fit the measured data well. No one method is foolproof, and multiple methods used in harmony yield the best confidence for accurately estimating the critical speed.

References

1. Wagner, E. R., Holzinger, D. W., and Nagele, F. C., "Critical Speed," Chap. 10 in *Universal Joint and Driveshaft Design Manual*, Advances in Engineering Series. No. 7, The Society of Automotive Engineers, Inc., ISBN 0-89883-007-9, 1991.
2. Adams, Maurice L., *Rotating Machinery Vibration: From Analysis to Troubleshooting*, 2nd Ed., CRC Press, ISBN 978-1-4398-0717-0, 2010.
3. Den Hartog, J. P., *Mechanical Vibrations*, Dover Publications, Inc, ISBN 0-486-64785-4, New York, 1985.
4. Shigley, Joseph Edward, *Dynamic Analysis of Machines*, McGraw-Hill, New York, 1961.
5. Periat and Hickey, "Critical Speed Failure Mode of a Steel Driveshaft," SAE Technical Paper 982764, ISBN 0148-7191, 1998.
6. Foulkes, Martin G., De Clerck, James P., and Singh, Rajendra, "Vibration Characteristics of Cardboard Inserts in Shells," SAE Technical Paper 2003-01-1489, 2003.
7. Clough, Ray W. and Penzien, Joseph, *Dynamics of Structures*, 2nd Ed., McGraw-Hill, ISBN 0-07-011394-7, 1993.
8. Juvinall, Robert C., *Fundamentals of Machine Component Design*, John Wiley & Sons, ISBN 0-471-06485-8, 1983.
9. Young, Warren C., *Roark's Formulas for Stress and Strain*, 6th Ed., McGraw-Hill, ISBN 0-07-072541-1, 1989.
10. Xia, et al. "Study on the Bending Vibration of a Two-Piece Propeller Shaft for 4WD Driveline," SAE Technical Paper 2015-01-2174, 2015, DOI: 10.4271/2015-01-2174. 

The author can be reached at: whiterobertj@johndeere.com.